the FEBS Journal

# A natural osmolyte trimethylamine *N*-oxide promotes assembly and bundling of the bacterial cell division protein, FtsZ and counteracts the denaturing effects of urea

Arnab Mukherjee, Manas K. Santra, Tushar K. Beuria and Dulal Panda

School of Biosciences and Bioengineering, Indian Institute of Technology Bombay, Mumbai, India

**Keywords**
FtsZ; FtsZ unfolding; osmolyte; protofilaments bundling; TMAO

**Correspondence**
D. Panda, School of Biosciences and Bioengineering, Indian Institute of Technology Bombay, Powai, Mumbai 400076, India
Fax: +91 22 2572 3480
Tel: +91 22 2576 7838
E-mail: panda@iitb.ac.in

(Received 27 December 2004, revised 24 February 2005, accepted 1 April 2005)

doi:10.1111/j.1742-4658.2005.04696.x

Assembly of FtsZ was completely inhibited by low concentrations of urea and its unfolding occurred in two steps in the presence of urea, with the formation of an intermediate [Santra MK & Panda D (2003) *J Biol Chem* **278**, 21336–21343]. In this study, using the fluorescence of 1-anilininonaphthalene-8-sulfonic acid and far-UV circular dichroism spectroscopy, we found that a natural osmolyte, trimethylamine *N*-oxide (TMAO), counteracted the denaturing effects of urea and guanidium chloride on FtsZ. TMAO also protected assembly and bundling of FtsZ protofilaments from the denaturing effects of urea and guanidium chloride. Furthermore, the standard free energy changes for unfolding of FtsZ were estimated to be 22.5 and 28.4 kJ·mol$^{-1}$ in the absence and presence of 0.6 M TMAO, respectively. The data are consistent with the view that osmolytes counteract denaturant-induced unfolding of proteins by destabilizing the unfolded states. Interestingly, TMAO was also found to affect the assembly properties of native FtsZ. TMAO increased the light-scattering signal of the FtsZ assembly, increased sedimentable polymer mass, enhanced bundling of FtsZ protofilaments and reduced the GTPase activity of FtsZ. Similar to TMAO, monosodium glutamate, a physiological osmolyte in bacteria, which induces assembly and bundling of FtsZ filaments *in vitro* [Beuria TK, Krishnakumar SS, Sahar S, Singh N, Gupta K, Meshram M & Panda D (2003) *J Biol Chem* **278**, 3735–3741], was also found to counteract the deleterious effects of urea on FtsZ. The results together suggested that physiological osmolytes may regulate assembly and bundling of FtsZ in bacteria and that they may protect the functionality of FtsZ under environmental stress conditions.

Organisms, including bacteria, store a number of different small organic molecules called 'osmolytes' to counteract environmental stresses, including osmotic stresses, like temperature, cellular dehydration, desiccation, high extracellular salt environments and denaturants [1–3]. The counteracting effects of osmolytes against the deleterious effects of denaturants on proteins are widely thought to be due to the unfavorable transfer free energy of the peptide backbone from water to osmolyte, which preferentially destabilizes the unfolded states of the protein [4,5]. Osmolytes are generally subdivided into three chemical classes, namely polyols, amino acids and methylamines. Trimethylamine *N*-oxide (TMAO), a member of the methylamine class, is commonly found in the tissues of marine organisms [1,6,7], e.g. coelacanth and elasmobranches

**Abbreviations**
ANS, 1-anilinonaphthalene-8-sulfonic acid; CD, circular dichroism; GdnHCl, guanidium chloride; TMAO, trimethylamine *N*-oxide; TNP-GTP, 2′-(or-3′)-*O*-(trinitrophenyl) guanosine 5′-triphosphate trisodium salt.

[3,8]. High intracellular levels of TMAO in polar fish are believed to increase the osmotic concentrations that decrease the freezing point of body fluids [9,10]. TMAO also counteracts the deleterious effect of hydrostatic pressure on enzyme activity in deep-sea animals [11–14]. TMAO is derived from the trimethyl ammonium group of choline [7]. Dietary choline is oxidized to trimethylamine by bacteria and trimethylamine undergoes further oxidation to form TMAO [15–17]. TMAO has been shown to offset the denaturing effects of chemical denaturants on several proteins [6,18–21]. For example, TMAO was found to restore the polymerization ability of tubulin in the presence of a high concentration of urea [21]. The counteracting ability of an osmolyte was also found to vary from protein to protein [21,22]. In addition to their counteracting effects on protein unfolding, osmolytes can affect the functional properties of proteins. For example, TMAO has been shown to enhance assembly of the eukaryotic cytoskeletal protein, tubulin [21].

The prokaryotic homolog of tubulin, FtsZ, plays an important role in bacterial cell division [23–27]. FtsZ has several properties in common with the cytoskeleton protein tubulin [25–28]. Like tubulin, FtsZ assembles to form filamentous polymers in a GTP-dependent manner [29–32]. Several factors are found to affect FtsZ assembly and the bundling of protofilaments *in vitro* [33–38]. Purified FtsZ monomers polymerize into single-stranded protofilaments with little or no bundling of protofilaments in an assembly reaction that is believed to be isodesmic in nature [39]. However, in the presence of divalent calcium, monosodium glutamate, ruthenium red and DEAE-dextran, FtsZ protofilaments associate into long rod-shaped or tubular polymers that become extensive bundles [33–37]. The bundling of FtsZ protofilaments is thought to play a key role in the formation and functioning of the cytokinetic Z-ring during septation [23,38,40–44]. The assembly properties of FtsZ were found to be extremely sensitive to low concentrations of denaturants like urea, guanidium chloride (GdnHCl) [45]. Furthermore, the loss of functional properties of FtsZ preceded the global unfolding of FtsZ [45]. Although urea- and GdnHCl-induced unfolding of FtsZ were found to be highly reversible [45,46], the unfolding of tubulin was found to be irreversible in the absence of a chaperone [46,47].

In this study, we investigated the counteracting effects of two natural osmolytes namely TMAO and monosodium glutamate against the denaturing effects of urea on the bacterial cell division protein, FtsZ. TMAO was chosen because of its ability to counteract the denaturing effects of urea on tubulin [21], the eukaryotic homolog of FtsZ [23–26]. Monosodium glutamate is one of the common physiological osmolytes in bacteria [48]. It enhances assembly and bundling of FtsZ and stabilizes FtsZ polymers [33]. In this study, we found that TMAO and monosodium glutamate counteracted the denaturing effects of urea on FtsZ. Interestingly TMAO also enhanced the bundling of FtsZ protofilaments and suppressed GTPase activity of native FtsZ suggesting that osmolytes can modulate assembly and bundling of FtsZ protofilaments. The results also indicate that osmolytes can counteract FtsZ destabilizing forces in bacteria under environmental stress.

## Results

### Urea-induced FtsZ unfolding in the presence and absence of TMAO monitored by 1-anilinonaphthalene-8-sulfonic acid fluorescence

FtsZ (2.4 μM) was incubated with different concentrations of urea (0–8 M) in the absence and presence of 0.6 M TMAO for 30 min at 25 °C. The fluorescence intensities of the protein solutions were measured after an additional 30 min incubation with 50 μM 1-anilinonaphthalene-8-sulfonic acid (ANS). Similar to a previous report [45], we found that urea-induced unfolding of FtsZ occurred in two steps in the absence of TMAO (Fig. 1). Although the unfolding isotherm remained

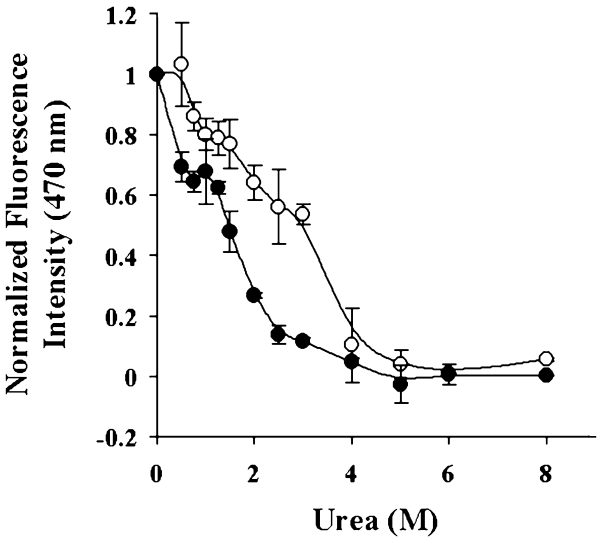


**Fig. 1.** Effects of TMAO on urea-induced unfolding of FtsZ. FtsZ (2.4 μM) was incubated with different concentrations (0–8 M) of urea in the absence (●) and presence (○) of 0.6 M TMAO for 30 min at 25 °C in 25 mM sodium phosphate buffer, pH 7. Then, 50 μM ANS was added and the mixtures were incubated for an additional 30 min. The fluorescence intensities of the solutions were recorded at 470 nm using 360 nm as an excitation wavelength. Data are averages of four independent experiments. Error bars represent SD.

**Table 1.** The $\Delta G$-values of urea-induced unfolding reaction of FtsZ (monitored by ANS fluorescence). The $\Delta G_{total}$ for each concentration of urea was calculated by adding $\Delta G_{N\rightarrow I}$ and $\Delta G_{I\rightarrow U}$.

| | Absence of TMAO | | | Presence of 0.6 M TMAO | | |
|---|---|---|---|---|---|---|
| Urea (M) | $\Delta G_{N\rightarrow I}$ (kJ·mol$^{-1}$) | $\Delta G_{I\rightarrow U}$ (kJ·mol$^{-1}$) | $\Delta G_{total}$ (kJ·mol$^{-1}$) | $\Delta G_{N\rightarrow I}$ (kJ·mol$^{-1}$) | $\Delta G_{I\rightarrow U}$ (kJ·mol$^{-1}$) | $\Delta G_{total}$ (kJ·mol$^{-1}$) |
| 0 | 10.5 | 12.0 | 22.5 | 12.7 | 15.7 | 28.4 |
| 0.25 | 3.1 | 10.4 | 13.5 | 8.1 | 14.4 | 22.5 |
| 0.5 | −4.4 | 8.9 | 4.5 | 3.6 | 13.2 | 16.8 |
| 0.75 | −11.8 | 7.3 | −4.5 | −0.9 | 12.0 | 11.1 |
| 1.0 | −19.2 | 5.7 | −13.5 | −5.4 | 10.7 | 5.3 |
| 1.25 | −26.6 | 4.1 | −22.5 | −10.0 | 9.4 | −0.6 |
| 1.5 | −34.0 | 2.6 | −31.4 | −14.6 | 8.2 | −6.4 |
| 2.0 | −48.9 | −0.5 | −49.4 | −23.7 | 5.7 | −18.0 |
| 2.5 | −63.7 | −3.6 | −67.3 | −32.8 | 3.2 | −29.6 |
| 3.0 | −78.6 | −6.7 | −85.3 | −41.9 | 0.7 | −41.2 |
| 4.0 | −108.2 | −13.0 | −121.2 | −60.1 | −4.2 | −64.3 |
| 5.0 | −137.9 | −19.2 | −157.1 | −78.3 | −9.2 | −87.5 |
| 6.0 | −167.6 | −25.4 | −193.0 | −96.5 | −14.2 | −110.7 |

biphasic in the presence of 0.6 M TMAO, higher concentrations of urea were required to induce similar levels of unfolding in presence of the osmolyte compared with the control. For example, 50% loss of ANS fluorescence intensity occurred at 1.5 and 3 M urea in the absence and presence of 0.6 M TMAO, respectively (Fig. 1). The results indicated that TMAO strongly counteracted urea-induced unfolding of FtsZ.

The free energy changes ($\Delta G$) of the unfolding of FtsZ were calculated at varying urea concentrations in the absence and presence of 0.6 M TMAO as described in Experimental procedures. Table 1 shows the estimated $\Delta G$ values of FtsZ unfolding steps in the presence of different urea concentrations. The results indicated that the transition from the native to the intermediate step ($\Delta G_{N\rightarrow I}$) of the urea-induced unfolding of FtsZ was more favorable process than the transition from the intermediate to the unfolded state ($\Delta G_{I\rightarrow U}$) of the protein. For example, in the presence of 0.25 M urea $\Delta G_{N\rightarrow I}$ and $\Delta G_{I\rightarrow U}$ are 3.1 and 10.4 kJ·mol$^{-1}$, respectively. The total $\Delta G$ ($\Delta G_{total}$) of FtsZ unfolding was obtained by adding the free energy changes from the native to intermediate ($\Delta G_{N\rightarrow I}$) and intermediate to unfolded state ($\Delta G_{I\rightarrow U}$). A plot of $\Delta G_{total}$ against urea concentrations yielded $x$-axis intercepts of 0.6 and 1.25 M urea in the absence and presence of 0.6 M TMAO, respectively (plot not shown). The finding suggested the urea-induced unfolding of FtsZ occurred spontaneously at urea concentrations $> 0.6$ M and $> 1.25$ M in the absence and presence of 0.6 M TMAO, respectively. Furthermore, the standard free energy changes of unfolding of FtsZ (at zero urea concentration) were found to be 22.5 and 28.4 kJ·mol$^{-1}$ in the absence and presence of 0.6 M TMAO, respectively. The higher $\Delta G°$ of unfolding in TMAO compared with water may be due to destabilization of the unfolded state in TMAO (see Discussion).

TMAO also reduced the FtsZ–ANS fluorescence in a concentration-dependent fashion. For example, FtsZ–ANS fluorescence was reduced by 15, 37, 45 and 55% in the presence of 0.2, 0.4, 0.6 and 0.8 M TMAO, respectively. Although the intensity of the FtsZ–ANS complex was found to decrease with increasing TMAO concentration, the anisotropy of the FtsZ–ANS complex did not reduce with the increasing concentration of TMAO. For example, the anisotropy of the FtsZ–ANS complex was found to be 0.19 both in the absence and presence of 0.8 M TMAO (data not shown). Thus, the reduction in the fluorescence intensity of the FtsZ–ANS complex with increasing concentration of TMAO was not due a reduction in the binding affinity of ANS to FtsZ but due conformational change in the protein.

## TMAO reversed denaturant-induced loss of secondary structure of FtsZ

TMAO (0.8 M) had minimal effects on the secondary structure of native FtsZ (Fig. 2A). FtsZ lost 85% of its secondary structure in the presence of 3 M urea. TMAO reversed the loss of the secondary structure in a concentration-dependent fashion (Fig. 2A). For example, 84% of the original secondary structure was recovered in the presence of 0.8 M TMAO. The far-UV circular dichroism (CD) (222 nm) signal of FtsZ in the absence and presence of 0.8 M TMAO with increasing concentration of urea are shown in Fig. 2B. Consistent with a previous report [45], the secondary structure of FtsZ appeared to decrease in one step with increasing concentration of urea in the absence and presence of TMAO. The $D_m$ values for the urea-induced unfolding of FtsZ were found to be 1.8 and 3.6 M in the absence and presence of TMAO, respectively. Furthermore, TMAO also inhibited the GdnHCl-induced perturbation of the secondary structures of FtsZ (Fig. 2C). Taken together the results suggested that TMAO strongly counteracted the denaturing activities of urea and GdnHCl on FtsZ (Figs 1 and 2).

## TMAO suppressed urea-induced inhibition of FtsZ assembly

Low urea concentrations strongly inhibited assembly of FtsZ [45]. TMAO counteracted the denaturing effects of urea on FtsZ (Figs 1 and 2). Thus, we wanted to know whether TMAO could reverse the

inhibitory effects of urea on FtsZ assembly. FtsZ (7.3 μM) was incubated with 0.2 M urea in the absence and presence of different concentrations of TMAO for 30 min at room temperature. After 30 min incubation, 10 mM $CaCl_2$, 10 mM $MgCl_2$ and 1 mM of GTP were added to the reaction mixture. The assembly of FtsZ was followed by light scattering. Urea (0.2 M) completely inhibited the assembly of FtsZ (Fig. 3A). Light scattering traces showed that TMAO inhibited the effect of urea in concentration dependent manner (Fig. 3A). For example, 0.4 and 0.6 M TMAO reversed the inhibitory effects of 0.2 M urea on the assembly of FtsZ by 47 and 55%, respectively (Fig. 3A).

Furthermore, a low concentration (0.125 M) of GdnHCl strongly inhibited FtsZ polymerization [45]. Similar to its ability to counteract the inhibitory effects of urea on FtsZ assembly, TMAO (0.6 M) reversed the inhibitory effects of GdnHCl on FtsZ assembly (Fig. 3B). The results indicated that TMAO could protect FtsZ from the deleterious effects of urea and GdnHCl.

### Effects of TMAO on FtsZ assembly

TMAO increased the light-scattering signal of FtsZ assembly in a concentration-dependent manner (Fig. 4). For example, 0.8 M TMAO increased the light-scattering intensity around fivefold from 45 to 220 a.u. (arbitrary unit). The slow increase in the light-scattering signal in the presence of TMAO indicated bundling of FtsZ protofilaments. TMAO also increased the sedimentable polymer mass of FtsZ assembly (Fig. 5). For example, 64 and 82% of the total FtsZ were pelleted in the absence and presence of 0.8 M TMAO, respectively. Electron microscopy analysis of the FtsZ assembly reaction showed the formation of thicker and larger bundles of FtsZ protofilaments in the presence of TMAO compared with the control (Fig. 6). The widths of the bundles of FtsZ

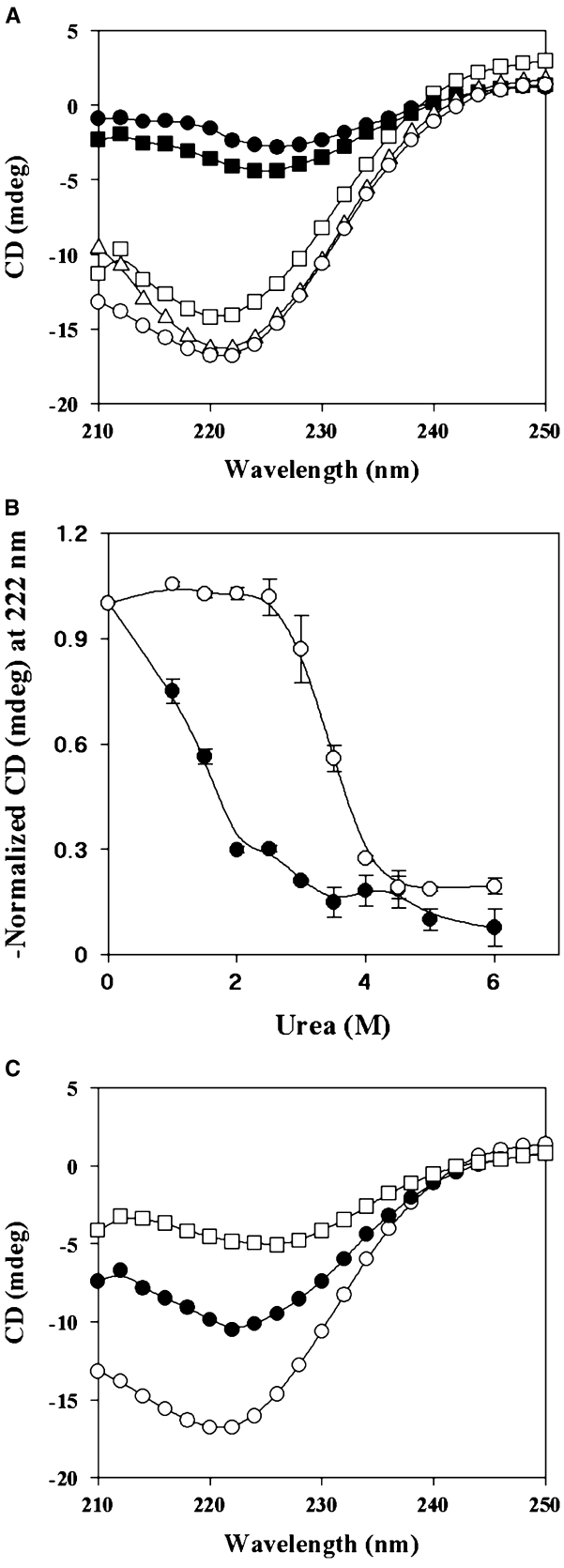


**Fig. 2.** Effects of TMAO on denaturant-induced perturbation of the far-UV CD spectra of FtsZ. FtsZ (7.3 μM) was incubated with 3 M urea in the absence and presence of different concentrations of TMAO for 30 min at 25 °C in 25 mM phosphate buffer, pH 7. The secondary structures of FtsZ were monitored over the wavelength range 200–250 nm using a 0.1 cm path length cuvette. (A) Far UV-CD spectra of the following solutions: control (△), 3 M urea (●), 3 M urea and 0.4 M TMAO (■), 3 M urea and 0.8 M TMAO (□), 0.8 M TMAO only (○). (B) Normalized CD values at 222 nm are plotted against different concentration (0–6 M) of urea in the absence (●) and presence (○) of 0.8 M TMAO. (C) Far UV-CD spectra of FtsZ under different conditions namely control (○), 1.5 M GdnHCl (□), 1.5 M GdnHCl and 0.8 M TMAO (●).

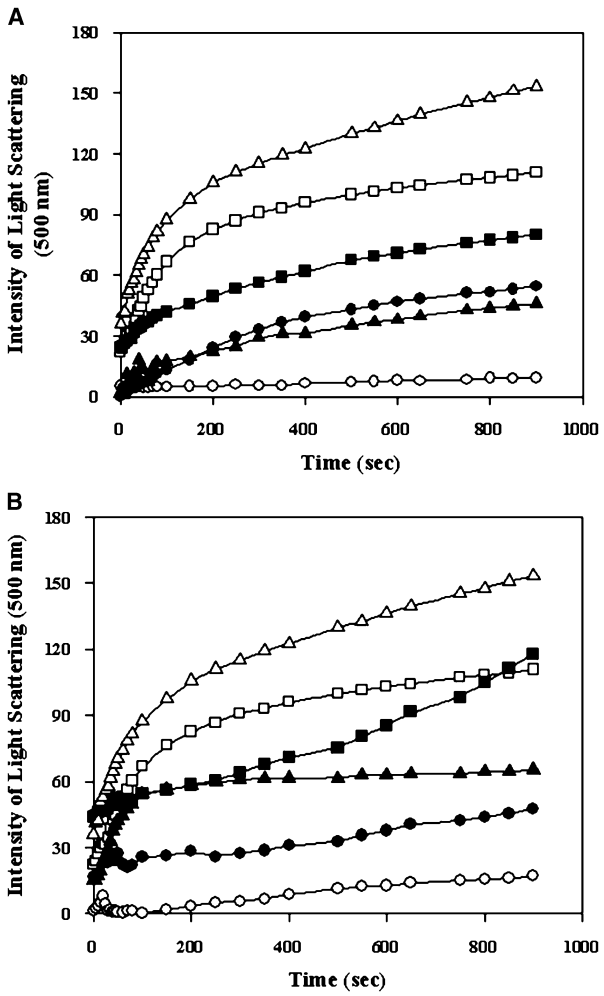


**Fig. 3.** Effects of TMAO on denaturant-inhibited assembly of FtsZ. FtsZ (7.3 μM) was assembled in the presence of 1 mM GTP, 10 mM $CaCl_2$, 10 mM $MgCl_2$. Urea (0.2 M) and TMAO (0.4 and 0.6 M) were added to different aliquots of FtsZ solutions prior to the addition of 10 mM $MgCl_2$, 10 mM $CaCl_2$ and 1 mM GTP. (A) Light-scattering traces of the assembly kinetics of FtsZ of the following solution conditions, control (▲), 0.2 M urea (○), and 0.2 M urea plus varying concentrations [0.4 M (●), 0.6 M (■)] of TMAO. Data are compared with 0.4 M (□), 0.6 M (△) of TMAO. (B) Time course FtsZ assembly of the following solution conditions, control (▲), 0.125 M GdnHCl (○) and 0.125 M GdnHCl along with 0.4 M (●), 0.6 M (■). Data are compared with 0.4 M (□), 0.6 M (△) TMAO.

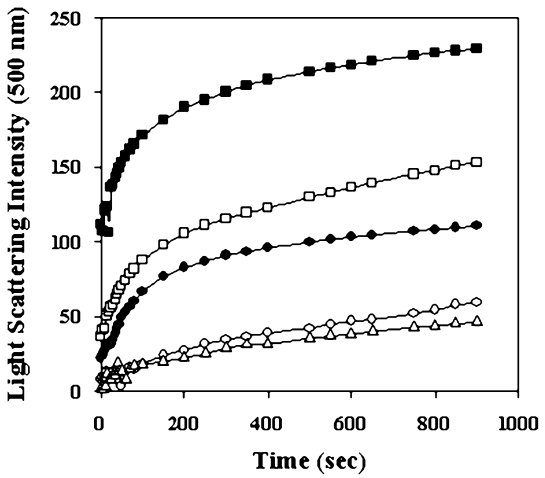


**Fig. 4.** Effects of TMAO on the calcium-induced assembly of FtsZ. FtsZ (7.3 μM) was incubated different concentrations of TMAO for 20 min at 25 °C. The assembly of FtsZ was initiated by adding 10 mM $CaCl_2$, 10 mM $MgCl_2$, 1 mM GTP to the reaction mixtures and the assembly reaction was immediately monitored at 37 °C. The traces represent FtsZ assembly kinetics of control (△) and different concentrations 0.2 M (○), 0.4 M (●), 0.6 M (□), and 0.8 M (■) TMAO.

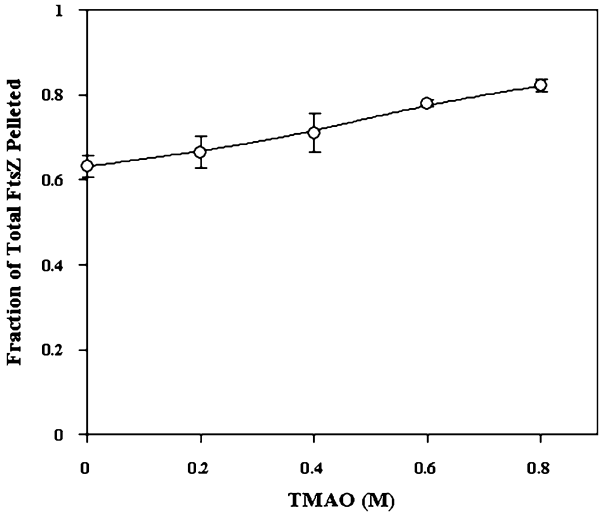


**Fig. 5.** Effects of TMAO on the sedimentable polymer mass of FtsZ. FtsZ (7.3 μM) was assembled in the presence of varying concentrations of TMAO as described in Fig. 4. The protein concentrations in the pellets were quantified as described in Experimental procedures. The experiment was performed five times. Error bars represent SD.

protofilaments were 37 ± 6 and 59 ± 9 nm in the absence and presence of 0.8 M TMAO, respectively (Fig. 6). Taken together, these results indicated that TMAO increased the light-scattering signal of the assembly reaction and sedimentable polymer mass by enhancing the formation of larger bundles of FtsZ protofilaments.

The previous experiments (Figs 4–6) were carried out using assembly milieu containing divalent calcium, which induces the bundling of protofilaments [33,34]. Thus, we wanted to know whether TMAO could induce bundling of FtsZ protofilaments in the absence of divalent calcium. TMAO enhanced

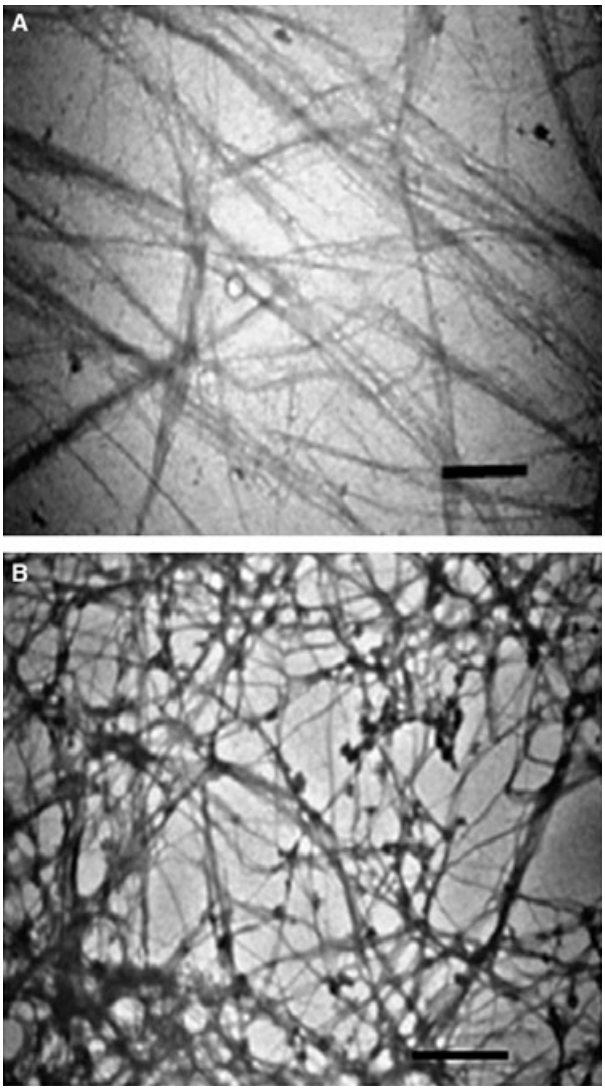


**Fig. 6.** Electron micrographs of calcium-induced FtsZ polymers in the absence (A) and presence (B) of 0.8 M TMAO. FtsZ (7.3 μM) was assembled in the presence of 10 mM of divalent calcium, 10 mM $MgCl_2$ and 1 mM GTP without or with 0.8 M TMAO as described in Experimental procedures. In all cases, the bar scale is 1000 nm.

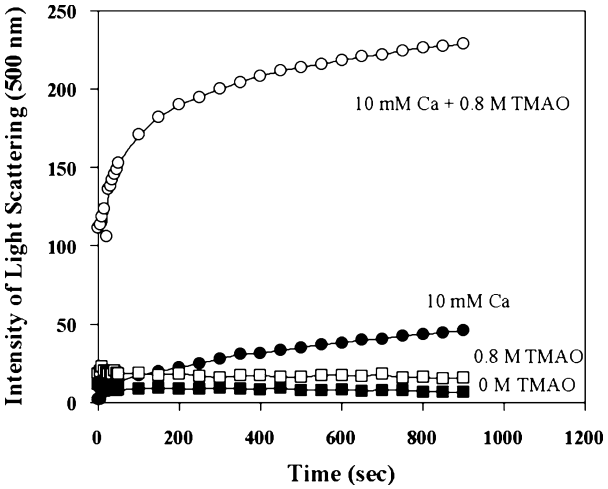


**Fig. 7.** Assembly of FtsZ in the presence of TMAO. FtsZ (7.3 μM) was incubated in the absence (■) and presence of 0.8 M (□) TMAO for 20 min. The polymerization of FtsZ was initiated by adding 10 mM $MgCl_2$ and 1 mM GTP and the reaction was monitored at 37 °C. Divalent calcium was not added in the reaction milieu. Light-scattering traces of FtsZ assembly in the presence of 10 mM calcium plus 0.8 M TMAO (○) and 10 mM $CaCl_2$ (●) are shown. Experiments were performed three times.

the light-scattering signal of FtsZ assembly minimally in the absence of calcium indicating its inability to induce bundle formation (Fig. 7). Furthermore, TMAO did not increase the sedimentable polymeric mass of FtsZ significantly. For example, 26 and 33% of the total FtsZ formed sedimentable polymers in the absence and presence of 0.8 M TMAO. Electron microscopy analysis showed that TMAO predominantly induced aggregation of FtsZ monomers in the absence of calcium (data not shown). Thus, the results suggested that TMAO cannot induce bundling of FtsZ by itself but it can enhance bundling of assembled protofilaments.

In the absence of added GTP, TMAO enhanced the light-scattering signal of the FtsZ assembly in a concentration-dependent manner if divalent calcium were present in the reaction mixture (Fig. 8A). FtsZ predominantly formed aggregates under these conditions; however, a few filamentous polymers were also observed (Fig. 8B). The results indicated that GTP is required for the formation of filamentous polymers. TMAO also reduced the rate of GTP hydrolysis of FtsZ in a concentration dependent manner (Fig. 9). For example, the hydrolysis rate was reduced by 20 and 40% in the presence of 0.4 and 0.8 M TMAO, respectively. In addition, TMAO (0.8 M) was found to reduce the binding of 2′-(or-3′)-*O*-(trinitrophenyl) guanosine 5′-triphosphate trisodium salt (TNP-GTP; an analog of GTP) to FtsZ. For example, the incorporation ratio of TNP-GTP per FtsZ monomer was found to be $0.84 \pm 0.04$ and $0.66 \pm 0.05$ in the absence and presence of 0.8 M TMAO, respectively. The reduction in the GTPase activity of FtsZ in the presence of TMAO may be partly due to the solvophobic effects of TMAO on FtsZ that reduces the binding of GTP to FtsZ. TMAO enhanced aggregation of FtsZ that could also reduce the GTPase activity of FtsZ.

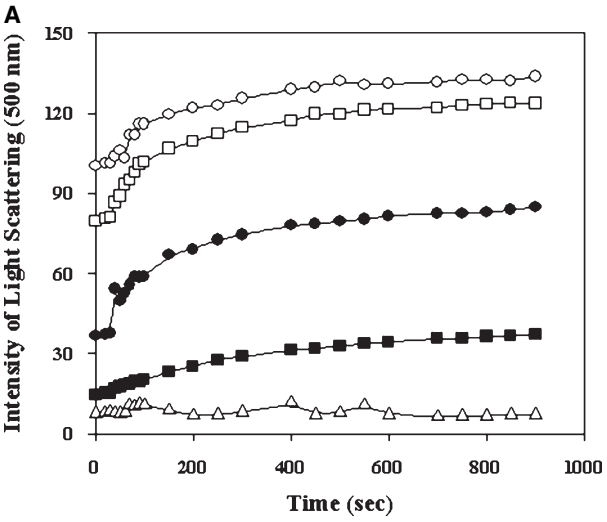


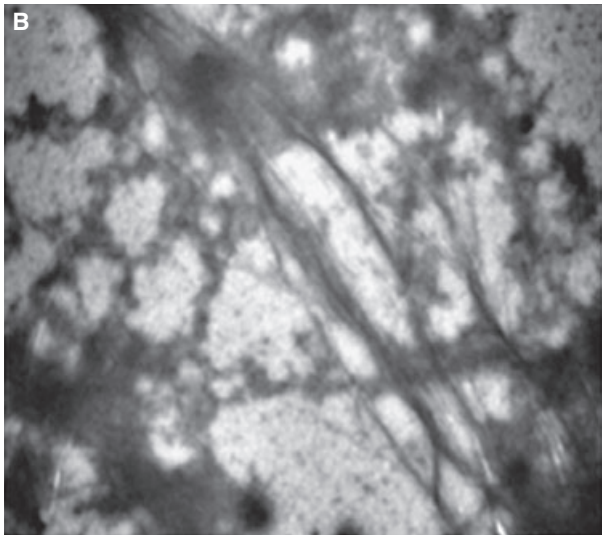


**Fig. 8.** Association of FtsZ monomers in increasing concentrations of TMAO in the absence of GTP. FtsZ (7.3 μM) was incubated with 10 mM $CaCl_2$ and 10 mM $MgCl_2$ without (△) or with different concentrations: 0.2 M (■), 0.4 M (●), 0.6 M (□), 0.8 M (○) of TMAO (A). (B) Electron micrograph of FtsZ polymers formed in the presence of 10 mM $CaCl_2$, 10 mM $MgCl_2$ and 0.8 M TMAO.

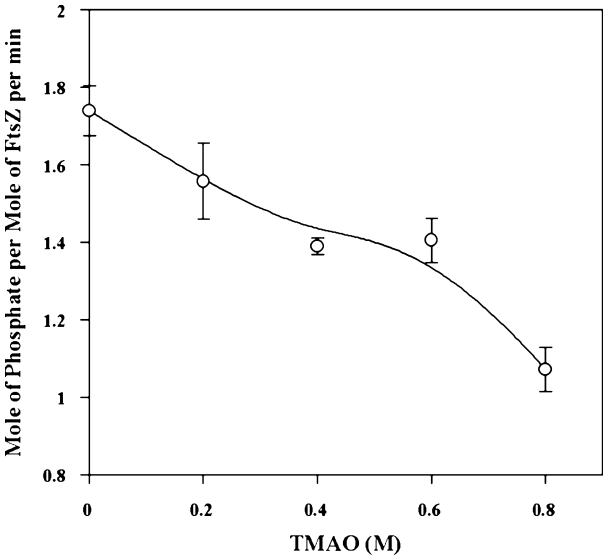


**Fig. 9.** Effects of TMAO on the GTPase activity of FtsZ. FtsZ (7.3 μM) was incubated in the absence and presence of different concentrations of TMAO (0.2–0.8 M) for 20 min. The rate of phosphate release per mol of FtsZ was determined as described in Experimental procedures. Data are averages of four individual experiments. Error bars represent SD.

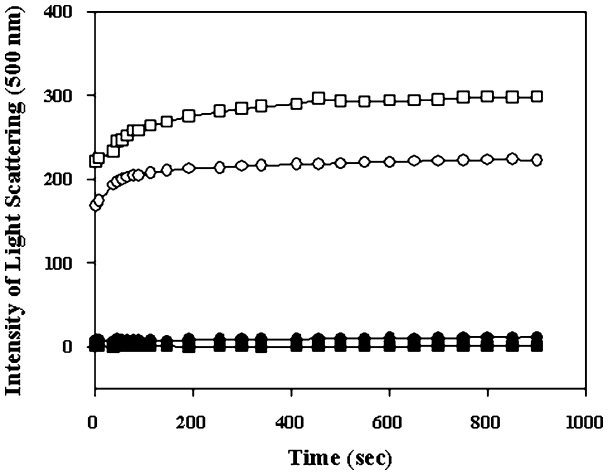


**Fig. 10.** Counteracting affects of monosodium glutamate on the inhibitory effects of urea on the assembly of FtsZ. FtsZ (7.3 μM) was assembled in the presence of 1 mM GTP and 10 mM $MgCl_2$ at 37 °C with following solution conditions: presence of 1 M glutamate (□), no glutamate (●), 0.25 M urea (■) and 1 M glutamate plus 0.25 M urea (○). Traces are provided from one of the three similar experiments.

## Glutamate reversed urea-induced inhibition of FtsZ assembly

Glutamate, a physiological osmolyte, has been shown to induce assembly and bundling of FtsZ protofilaments *in vitro* [33]. Urea (0.25 M) inhibited the light-scattering signal of the glutamate-induced assembly of FtsZ by 22% (Fig. 10). Glutamate-induced assembly of FtsZ produced 290 a.u. of light scattering in the absence of urea, and 225 a.u. of light scattering in the presence of 0.25 M urea (Fig. 10). However, urea (0.2 M) completely inhibited calcium-induced assembly of FtsZ (Fig. 3A). Thus, like TMAO, glutamate prevents the inhibitory effects of urea on FtsZ assembly.

## Discussion

Two natural osmolytes, TMAO and monosodium glutamate, were found to offset the denaturing effects of urea and GdnHCl on FtsZ *in vitro* indicating that osmolytes could counteract the deleterious effects of environmental stresses on FtsZ assembly and bundling in bacteria. TMAO (0.6 M) increased the $D_m$ (urea concentration required to unfold FtsZ by 50%) value of urea-induced unfolding of FtsZ by twofold from 1.5 to 3 M urea. An estimation of the free energy changes of the urea-induced unfolding reaction showed that FtsZ unfolds spontaneously at lower concentrations of urea in the absence of TMAO than its presence (Table 1). Furthermore, $\Delta G°$ of FtsZ unfolding was determined to be 22.5 kJ·mol$^{-1}$ in water and 28.4 kJ·mol$^{-1}$ in 0.6 M TMAO. The higher $\Delta G°$ of unfolding of FtsZ in TMAO compared with water suggested that the counteractive effects of TMAO on urea-induced unfolding of FtsZ could be due to either stabilization of the native state or destabilization of the unfolded state. It has been shown that the transfer of a native protein from water to an osmolyte solution increases the Gibb's free energy [4,5,49]. It is widely argued that the counteracting ability of the osmolyte does not arise from the stabilization of the native state but arises primarily from the destabilization of the unfolded state of the protein in the presence of osmolyte [4,5,49,50]. Thus, the counteractive effect of TMAO on FtsZ unfolding is likely due to destabilization of the unfolded state of the protein in TMAO compared with water. However, TMAO assisted bundling of FtsZ protofilaments indicating that FtsZ may adopt a conformation in osmolyte solution that is different from its native state. The different conformation of FtsZ may contribute partly to its resistance against denaturant-induced unfolding.

Timasheff and coworkers also reported a similar mechanism to explain the counteracting abilities of osmolytes [51,52]. They suggested that due to the unfavorable interaction between osmolytes and protein, osmolytes are preferentially excluded from the immediate surroundings of the protein [51,52]. This type of distribution of solvent molecules in protein is entropically unfavorable and it becomes more unfavorable with increasing surface area of the protein. Osmolytes may decrease the solvent-accessible surface area of proteins and the reduction in the solvent-accessible surface area produces a decrease in the ligand-binding ability of the protein [52]. An unfavorable interaction between protein and osmolyte is commonly known as the solvophobic effect. Although TMAO reduced the fluorescence intensity of the FtsZ–ANS complex, it did not reduce the anisotropy of the FtsZ–ANS complex. Thus, the reduction in the fluorescence intensity of the FtsZ–ANS complex was not due to a decrease in the binding ability of ANS to FtsZ, which ruled out a solvophobic effect as a cause of the reduction of ANS fluorescence in TMAO. The decrease in FtsZ–ANS fluorescence with increasing concentrations of TMAO may due to TMAO-induced conformational change in FtsZ which reduced the quantum yield of the bound FtsZ–ANS complex.

In addition to the counteracting effects of TMAO on FtsZ unfolding, TMAO was also found to affect FtsZ assembly. In the presence of divalent calcium, TMAO increased the light-scattering intensity of the assembly reaction, increased the sedimentable polymer mass and enhanced the extent of bundling of FtsZ protofilaments (Figs 4–6). Larger polymer bundles can scatter more light and can be pelleted more efficiently than thin protofilaments [35,53]. Thus, the increased light-scattering signals and sedimentable polymer mass in the presence of TMAO were most likely due to an increase in the bundling of the assembled protofilaments rather than to an actual increase in the assembled polymers. Interestingly, in the absence of calcium, TMAO failed to induce the bundling of FtsZ protofilaments (Fig. 7). The results suggested that TMAO could potentiate the bundling of FtsZ protofilaments, but alone could not induce bundling of the protofilaments. However, unlike TMAO, monosodium glutamate can induce and enhance the assembly and bundling of FtsZ protofilaments suggesting that different osmolytes can affect FtsZ assembly and bundling of protofilaments differently.

Bundling of FtsZ protofilaments plays important role in the formation and functioning of the cytokinetic Z-ring during bacterial cell division [38–40,54,55]. Although the mechanism of regulation of bundling is not clear, it is widely thought that bundling of protofilaments is a finely regulated process [54]. For example, EzrA binds to monomeric FtsZ and negatively regulates FtsZ assembly, which ensures that only one Z-ring is formed per cell cycle [38]. Furthermore, MinCDE (complex of MinC, MinD and MinE proteins) has been shown to inhibit bacterial cell division by preventing assembly of the Z-ring [23,40,55]. In addition to the proteinous regulation of bundling, it is likely that the bundling of protofilaments is regulated, at least in part, by small organic molecules and cations. In support of this, calcium and ruthenium red are shown to induce bundling of FtsZ protofilaments *in vitro* [34,35]. Furthermore, glutamate, an osmolyte commonly found in bacteria, also induces bundling of

FtsZ protofilaments *in vitro* [33]. The findings of this study suggest that physiological osmolytes may play a role in regulating the assembly dynamics of FtsZ in bacteria, at least in part, and they can protect FtsZ from environmental stresses.

## Experimental procedures

### Materials

TMAO was purchased from Fluka (Steinheim, Germany), Pipes was purchased from Sigma (Steinheim, Germany). GTP, GdnHCl and urea were purchased from Aldrich (Steinheim, Germany). TNP-GTP and ANS were purchased from Molecular Probes (Eugene, OR, USA). DE-52 was purchased from Whatman International Ltd (Maidstone, UK). All other reagents used were analytical grade.

### Protein purification

Recombinant *Escherichia coli* FtsZ was purified from *E. coli* BL21 strain using DE-52 ion exchange chromatography followed by a cycle of polymerization and depolymerization as described previously [33]. FtsZ concentration was measured by the method of Bradford using bovine serum albumin (BSA) as a standard [56]. FtsZ concentration was adjusted using a correction factor 0.82 for the FtsZ/BSA ratio [57]. Protein was frozen and stored at −80 °C.

### Preparation of denaturant solutions

The denaturant solutions (urea and GdnHCl) were prepared in 25 mM phosphate buffer, pH 7 for fluorescence and far UV-CD measurements. Urea and GdnHCl were dissolved in 25 mM Pipes, pH 6.8 for FtsZ assembly reactions. Final pH of the urea and GdnHCl solutions was adjusted using HCl and NaOH. Fresh solutions of urea and GdnHCl were used for all experiments.

### Spectroscopic methods

Fluorescence spectroscopic studies were performed using a JASCO FP-6500 fluorescence spectrophotometer (Tokyo, Japan). FtsZ (2.4 μM) was incubated with different concentrations of urea (0–8 M) in the absence and presence of 0.6 M TMAO for 30 min at 25 °C. The fluorescence intensities of the protein solutions were measured after an additional 30 min of incubation with 50 μM ANS. All spectra were corrected by subtracting the corresponding blank (without FtsZ) from the original spectra. The excitation and emission bandwidths were fixed at 5 and 10 nm, respectively. A quartz cuvette of 0.3 cm path length was used for all experiments except the anisotropy measurement where a cuvette of 1 cm path length was used. Emission spectra were recorded over the range of 425–550 nm using 360 nm as an excitation wavelength.

Fluorescence anisotropy studies were performed in a JASCO FP-6500 fluorescence spectrophotometer. FtsZ (7.3 μM) incubated with 50 μM ANS in the absence and presence of (0.5, 0.8 M) TMAO for 30 min at room temperature. The excitation and emission bandwidths were both fixed at 10 nm. A quartz cuvette of 1 cm path length was used for this experiment. Emission spectra were recorded over the range of 425–550 nm using 360 nm as an excitation wavelength.

CD studies were performed in a JASCO J810 spectropolarimeter equipped with a Peltier temperature controller. FtsZ (7.3 μM) was incubated with either urea or GdnHCl for 30 min at 25 °C in the absence and presence of TMAO. The secondary structure of FtsZ was monitored over the wavelength range of 200–250 nm using a 0.1 cm path length cuvette. Each spectrum was collected by averaging five scans. Each spectrum was corrected by subtracting appropriate blank spectrum containing no FtsZ from the experimental spectrum.

### Light-scattering assay

The polymerization reaction was monitored at 37 °C by light scattering at 500 nm using a JASCO 6500 fluorescence spectrophotometer. The excitation and emission wavelengths were 500 nm. The excitation and emission bandwidths used were 1 and 5 nm, respectively.

### Effect of TMAO on denaturant-induced inhibition of FtsZ polymerization

FtsZ (7.3 μM) in 25 mM pipes buffer, pH 6.8 was incubated with either 0.2 M urea or 0.125 M GdnHCl in the presence of different concentrations of TMAO (0–0.8 M) for 30 min at 25 °C. The polymerization reaction was initiated by adding 10 mM $MgCl_2$, 10 mM $CaCl_2$ and 1 mM GTP to the solution and immediately transferring the reaction mixtures to a cuvette at 37 °C.

### Effect of TMAO on FtsZ assembly and bundling

FtsZ (7.3 μM) in 25 mM Pipes (pH 6.8) was incubated in the absence and presence of different concentrations TMAO (0.2–0.8 M) for 20 min at 25 °C. The assembly reaction was initiated by adding 10 mM $MgCl_2$, 10 mM $CaCl_2$ and 1 mM GTP and immediately transferring the reaction mixtures to 37 °C. The kinetics of the assembly reaction was monitored by 90° light scattering at 500 nm [53].

The effects of TMAO on pelletable FtsZ polymer mass were quantified by sedimentation assay. FtsZ polymers were collected by sedimentation using 280 000 ***g*** for 20 min at 30 °C. Protein concentrations of the supernatants were

measured. Sedimentable polymeric mass of FtsZ was calculated by subtracting the supernatant concentration from the total protein concentration. Samples for electron microscopy were prepared as described previously [33]. Briefly, FtsZ polymers were fixed with 0.5% (v/v) glutaraldehyde and subsequently negatively stained with 2% (w/v) uranyl acetate. The electron micrographs were taken using a FEI TECNAI $G^2$12 cryo-electron microscope. All micrographs were taken at ×16 500 magnification. In all cases, bar = 1000 nm.

## Effect of glutamate on urea-induced inhibition of FtsZ assembly

FtsZ (7.3 μM) was incubated with 0.25 M urea in 25 mM Pipes pH 6.8 for 15 min at 25 °C. The polymerization reaction was initiated by adding 1 M glutamate, 10 mM $MgCl_2$ and 1 mM GTP and the intensity of light scattering was monitored for 15 min at 37 °C.

## Effect of TMAO on the GTPase activity of FtsZ

A standard malachite green ammonium molybdate assay was used to measure the production of inorganic phosphate during GTP hydrolysis [33,35,45,58]. Briefly, FtsZ (7.3 μM) was incubated with different concentrations of TMAO (0–0.8 M) in 25 mM Pipes (pH 6.8) at 25 °C for 20 min. Then, 5 mM $MgCl_2$ and 1 mM GTP were added to the reaction mixtures and incubated for an additional 15 min at 37 °C. After 15 min of hydrolysis, the reaction was quenched by adding 10% (v/v) 7 M perchloric acid. The quenched reaction mixtures were centrifuged for 5 min at 25 °C. The concentrations of inorganic phosphate in the supernatants were quantified using malachite green solution [33]. A standard curve for quantification of inorganic phosphate was prepared using sodium phosphate.

## GTP-binding measurement

TNP-GTP, an analog of GTP, was used to determine the stoichiometry of nucleotide binding to FtsZ in the absence and presence of TMAO. FtsZ (30 μM) was incubated with 100 μM TNP-GTP, 5 mM $Mg^{2+}$ in the absence and presence of 0.8 M TMAO for 4 h at room temperature. After 4 h of incubation, the protein solution was passed through a size-exclusion P-6 column (30 × 10 mm) to remove the free TNP-GTP. FtsZ-bound TNP-GTP concentration was determined by measuring its absorbance at 410 nm. FtsZ concentration was determined by the Bradford assay and corrected as described previously. The stoichiometry of nucleotide incorporation per FtsZ monomer was determined by dividing the bound TNP-GTP concentration by the protein concentration. The experiment was performed three times.

## Data analysis

Thermodynamic parameters of urea-induced unfolding process were determined using a three-state model [59–61]. The variation of fluorescence intensity of the FtsZ–ANS complex urea-induced denaturation of FtsZ was fitted in a three-state model 1 in the absence and presence of TMAO, respectively.

$$N \rightarrow I \rightarrow U \quad (1)$$

The free energy change from the native (N) to the unfolded state (U) through an intermediate state (I) was assumed to vary according to the empirical Eqn (2) [62,63],

$$\Delta G = \Delta G^0 - m[D] \quad (2)$$

Where, the $\Delta G$ is the free energy change at equilibrium from native to unfolded state at a particular denaturant concentration; the standard free energy change ($\Delta G°$) is the free energy change at zero denaturant concentration; [D] is the denaturant concentration and m is the corresponding slope of a plot $\Delta G$ against [D].

The values of $\Delta G°$ and $m$ were estimated by fitting the fluorescence or CD intensity ($S_{obs}$) against denaturant concentration, [D] in Eqn (3) for three state process [60],

$$S_{obs} = \frac{S_N + S_I \exp\{-(\Delta G_{N\rightarrow I} - m_{N\rightarrow I}[D])/RT\} + S_U \exp\{-(\Delta G_{N\rightarrow I} - m_{N\rightarrow I}[D])/RT\} \exp\{-\Delta G_{I\rightarrow U} - m_{I\rightarrow U}[D])/RT\}}{1 + \exp\{-(\Delta G_{N\rightarrow I} - m_{N\rightarrow I}[D])/RT\} + \exp\{-\Delta G_{N\rightarrow I} - m_{N\rightarrow I}[D])/RT\} \exp\{-\Delta G_{I\rightarrow U} - m_{I\rightarrow U}[D])/RT\}} \quad (3)$$

and Eqn (3a) [60] for two state process,

$$S_{obs} = \frac{S_N + S_U \exp\{-(\Delta G - m[D])/RT\}}{1 + \exp\{-(\Delta G - m[D])/RT\}} \quad (3a)$$

Where, $S_N$, $S_I$ and $S_U$ represent the intrinsic signal intensities of the native, intermediate and the unfolded states, respectively. $\Delta G_{N\rightarrow I}$ and $\Delta G_{I\rightarrow U}$ are the standard free energies for the N→I and I→U transitions and $m_{N\rightarrow I}$ and $m_{I\rightarrow U}$ are the $m$-values for the corresponding transitions, respectively. The data were fitted directly in Eqn (3) by nonlinear least squares analysis. The total free energy changes of FtsZ unfolding were determined by adding the $\Delta G_{N\rightarrow I}$ and $\Delta G_{I\rightarrow U}$.

## Acknowledgements

We thank Dr H. P. Erickson for providing us with the FtsZ clone. This study was supported by a grant from Department of Science and Technology, Government of India (to DP). MKS and TKB were supported by fellowships from the Council of Scientific and Industrial Research, Government of India.

## References

1 Yancey PH, Clark ME, Hand SC, Bowlus RD & Somero GN (1982) Living with water stress: evolution of osmolyte systems. *Science* **217**, 1214–1222.
2 Yancey PH & Somero GN (1979) Counteraction of urea destabilization of protein structure by methylamine osmoregulatory compounds of elasmobranch fishes. *Biochem J* **183**, 317–323.
3 Forster RP & Goldstein L (1976) Intracellular osmoregulatory role of amino acids and urea in marine elasmobranches. *Am J Physiol* **230**, 925–931.
4 Bolen DW (2001) Protein stabilization by naturally occurring osmolytes. *Methods Mol Biol* **168**, 17–36.
5 Bolen DW & Baskakov IV (2001) The osmophobic effect: natural selection of a thermodynamic force in protein folding. *J Mol Biol* **310**, 955–963.
6 Lange R & Fugelli K (1965) The osmotic adjustment in the euryhaline teleosts, the flounder, *Pleuronectes flesus* L. and the three-spined stickleback, *Gasterosteus aculeatus* L. *Comp Biochem Physiol* **15**, 283–292.
7 Seibel BA & Walsh PJ (2002) Trimethylamine oxide accumulation in marine animals: relationship to acylglycerol storage. *J Exp Biol* **205**, 297–306.
8 Somero GN (1986) From dogfish to dogs: trimethylamines protect proteins from urea. *News Physiol Sci* **1**, 9–12.
9 Raymond JA (1994) Seasonal variations of trimethylamine oxide and urea in the blood of a cold-adapted marine teleost, the rainbow smelt. *Fish Physiol Biochem* **13**, 13–22.
10 Raymond JA & DeVries AL (1998) Elevated concentrations and synthetic pathways of trimethylamine oxide and urea in some teleost fishes of McMurdo Sound, Antarctica. *Fish Physiol Biochem* **18**, 387–398.
11 Yancey PH & Siebenaller JF (1999) Trimethylamine oxide stabilizes teleost and mammalian lactate dehydrogenases against inactivation by hydrostatic pressure and trypsinolysis. *J Exp Biol* **202**, 3597–3603.
12 Yancey PH, Fyfe-Johnson AL, Kelly RH, Walker VP & Aunon MT (2001) Trimethylamine oxide counteracts effects of hydrostatic pressure on proteins of deep-sea teleosts. *J Exp Zool* **289**, 172–176.
13 Gillett MB, Suko JR, Santoso FO & Yancey PH (1997) Elevated levels of trimethylamine oxide in muscles of deep-sea gadiform teleosts: a high-pressure adaptation? *J Exp Zool* **279**, 386–391.
14 Kelly RH & Yancey PH (1999) High contents of trimethylamine oxide correlating with depth in deep-sea teleost fishes, skates and decapod crustaceans. *Biol Bull* **196**, 18–25.
15 Hebard CE, Flick GJ & Martin RE (1982) *Chemistry and Biochemistry of Marine Food Products*. AVI Publishing, Westport, CT.
16 Pierce SK, Dragolovich J & Crombie BN (1997) Variations in intracellular choline levels may account for differences in glycine betaine synthesis between conspecific oyster populations responding to hyperosmotic stress. *J Exp Zool* **278**, 283–289.
17 Ballantyne JS (1997) The inside story. The metabolism of elasmobranch fishes. *Comp Biochem Physiol* **118B**, 703–742.
18 Russo AT, Rosgen J & Bolen DW (2003) Osmolyte effects on kinetics of FKBP12 C22A folding coupled with prolyl isomerization. *J Mol Biol* **330**, 851–866.
19 Zou Q, Bennion BJ, Daggett V & Murphy KP (2002) The molecular mechanism of stabilization of proteins by TMAO and its ability to counteract the effects of urea. *J Am Chem Soc* **124**, 1192–1202.
20 Palmer HR, Bedford JJ, Leader JP & Smith RA (2000) $^{31}$P and $^{1}$H NMR studies of the effect of the counteracting osmolyte trimethylamine–*N*-oxide on interactions of urea with ribonuclease A. *J Biol Chem* **275**, 27708–27711.
21 Sackett DL (1997) Natural osmolyte trimethylamine *N*-oxide stimulates tubulin polymerization and reverses urea inhibition. *Am J Physiol* **273**, 669–676.
22 Mandal AK, Samaddar S, Banerjee R, Lahiri S, Bhattacharyya A & Roy S (2003) Glutamate counteracts the denaturing effect of urea through its effect on the denatured state. *J Biol Chem* **278**, 36077–36084.
23 Errington J, Daniel RA & Scheffers DJ (2003) Cytokinesis in bacteria. *Microbiol Mol Biol Rev* **67**, 52–65.
24 Lutkenhaus J (1993) FtsZ ring in bacterial cytokinesis. *Mol Microbiol* **9**, 403–409.
25 Lowe J & Amos LA (1998) Crystal structure of the bacterial cell-division protein FtsZ. *Nature* **391**, 203–206.
26 Nogales E, Wolf SG & Downing KH (1998) Structure of the alpha beta tubulin dimer by electron crystallography. *Nature* **391**, 199–203.
27 Rothfield LI & Justice SS (1997) Bacterial cell division: the cycle of the ring. *Cell* **88**, 581–584.
28 van den Ent F, Amos L & Lowe J (2001) Bacterial ancestry of actin and tubulin. *Curr Opin Microbiol* **4**, 634–638.
29 de Boer P, Crossley R & Rothfield L (1992) The essential bacterial cell-division protein FtsZ is a GTPase. *Nature* **359**, 254–256.
30 RayChaudhuri D & Park JT (1992) *Escherichia coli* cell-division gene *ftsZ* encodes a novel GTP-binding protein. *Nature* **359**, 251–254.
31 Mukherjee A, Dai K & Lutkenhaus J (1993) *Escherichia coli* cell division protein FtsZ is a guanine nucleotide

binding protein. *Proc Natl Acad Sci USA* **90**, 1053–1057.
32 Bramhill D & Thompson CM (1994) GTP-dependent polymerization of *Escherichia coli* FtsZ protein to form tubules. *Proc Natl Acad Sci USA* **91**, 5813–5817.
33 Beuria TK, Krishnakumar SS, Sahar S, Singh N, Gupta K, Meshram M & Panda D (2003) Glutamate-induced assembly of bacterial cell division protein FtsZ. *J Biol Chem* **278**, 3735–3741.
34 Yu XC & Margolin W (1997) $Ca^{2+}$-mediated GTP-dependent dynamic assembly of bacterial cell division protein FtsZ into asters and polymer networks *in vitro*. *EMBO J* **16**, 5455–5463.
35 Santra MK, Beuria TK, Banerjee A & Panda D (2004) Ruthenium red induced bundling of bacterial cell division protein, FtsZ. *J Biol Chem* **279**, 25959–25965.
36 Erickson HP, Taylor DW, Taylor KA & Bramhill D (1996) Bacterial cell division protein FtsZ assembles into protofilament sheets and minirings, structural homologs of tubulin polymers. *Proc Natl Acad Sci USA* **93**, 519–523.
37 Gonzalez JM, Jimenez M, Velez M, Mingorance J, Andreu JM, Vicente M & Rivas G (2003) Essential cell division protein FtsZ assembles into one monomer-thick ribbons under conditions resembling the crowded intracellular environment. *J Biol Chem* **278**, 37664–37671.
38 Haeusser DP, Schwartz RL, Smith AM, Oates ME & Levin PA (2004) EzrA prevents aberrant cell division by modulating assembly of the cytoskeletal protein FtsZ. *Mol Microbiol* **52**, 801–814.
39 Romberg L, Simon M & Erickson HP (2001) Polymerization of FtsZ, a bacterial homolog of tubulin. Is assembly cooperative? *J Biol Chem* **276**, 11743–11753.
40 Margolin W (2001) Spatial regulation of cytokinesis in bacteria. *Curr Opin Microbiol* **4**, 647–652.
41 Stricker J, Maddox P, Salmon ED & Erickson HP (2002) Rapid assembly dynamics of the *Escherichia coli* FtsZ-ring demonstrated by fluorescence recovery after photobleaching. *Proc Natl Acad Sci USA* **99**, 3171–3175.
42 RayChaudhuri D (1999) ZipA is a MAP-Tau homolog and is essential for structural integrity of the cytokinetic FtsZ ring during bacterial cell division. *EMBO J* **18**, 2372–2383.
43 Hale CA, Rhee AC & de Boer PA (2000) ZipA-induced bundling of FtsZ polymers mediated by an interaction between C-terminal domains. *J Bacteriol* **182**, 5153–5166.
44 Margolin W (2003) Bacterial division: the fellowship of the ring. *Curr Biol* **13**, R16–R18.
45 Santra MK & Panda D (2003) Detection of an intermediate during unfolding of bacterial cell division protein FtsZ: loss of functional properties precedes the global unfolding of FtsZ. *J Biol Chem* **278**, 21336–21343.
46 Andreu JM, Oliva MA & Monasterio O (2002) Reversible unfolding of FtsZ cell division proteins from archaea and bacteria. Comparison with eukaryotic tubulin folding and assembly. *J Biol Chem* **277**, 43262–43270.
47 Guha S & Bhattacharyya B (1997) Refolding of urea-denatured tubulin: recovery of native-like structure and colchicine binding activity from partly unfolded states. *Biochemistry* **36**, 13208–13213.
48 Record TM Jr, Courtenay ES, Cayley S & Guttman HJ (1998) Biophysical compensation mechanisms buffering *E. coli* protein–nucleic acid interactions against changing environments. *Trends Biochem Sci* **23**, 190–194.
49 Wang A & Bolen DW (1997) A naturally occurring protective system in urea-rich cells: mechanism of osmolyte protection of proteins against urea denaturation. *Biochemistry* **36**, 9101–9108.
50 Qu Y, Bolen CL & Bolen DW (1998) Osmolyte-driven contraction of a random coil protein. *Proc Natl Acad Sci USA* **95**, 9268–9273.
51 Arakawa T & Timasheff SN (1984) The mechanism of action of Na glutamate, lysine HCl, and piperazine-*N*,*N*′-bis (2-ethanesulfonic acid) in the stabilization of tubulin and microtubule formation. *J Biol Chem* **259**, 4979–4986.
52 Timasheff SN (2002) Protein–solvent preferential interactions, protein hydration, and the modulation of biochemical reactions by solvent components. *Proc Natl Acad Sci USA* **99**, 9721–9726.
53 Gaskin F, Cantor CR & Shelanski ML (1974) Turbidimetric studies of the *in vitro* assembly and disassembly of porcine neurotubules. *J Mol Biol* **89**, 737–755.
54 Koppelman CM, Aarsman ME, Postmus J, Pas E, Muijsers AO, Scheffers DJ, Nanninga N & den Blaauwen T (2004) R174 of *Escherichia coli* FtsZ is involved in membrane interaction and protofilament bundling, and is essential for cell division. *Mol Microbiol* **51**, 645–657.
55 Mazouni K, Domain F, Cassier-Chauvat C & Chauvat F (2004) Molecular analysis of the key cytokinetic components of cyanobacteria: FtsZ, ZipN and MinCDE. *Mol Microbiol* **52**, 1145–1158.
56 Bradford MM (1976) A rapid and sensitive method for the quantitation of microgram quantities of protein utilizing the principle of protein–dye binding. *Anal Biochem* **72**, 248–254.
57 Lu C, Stricker J & Erickson HP (1998) FtsZ from *Escherichia coli*, *Azotobacter vinelandii*, and *Thermotoga maritima* – quantitation, GTP hydrolysis, and assembly. *Cell Motil Cytoskeleton* **40**, 71–86.
58 Geladopoulos TP, Sotiroudis TG & Evangelopoulos AE (1991) A malachite green colorimetric assay for protein phosphatase activity. *Anal Biochem* **192**, 112–116.
59 Santoro MM & Bolen DW (1988) Unfolding free energy changes determined by the linear extrapolation method.

1. Unfolding of phenylmethanesulfonyl alpha-chymotrypsin using different denaturants. *Biochemistry* **27**, 8063–8068.
60 Bevinton PR (1969) *Data Reduction and Error Analysis for Physical Sciences*. McGraw-Hill, New York.
61 Pace CN, Laurents DV & Thomson JA (1990) pH dependence of the urea and guanidine hydrochloride denaturation of ribonuclease A and ribonuclease T1. *Biochemistry* **29**, 2564–2572.
62 Pace CN (1986) Determination and analysis of urea and guanidine hydrochloride denaturation curves. *Methods Enzymol* **131**, 266–280.
63 Morjana NA, McKeone BJ & Gilbert HF (1993) Guanidine hydrochloride stabilization of a partially unfolded intermediate during the reversible denaturation of protein disulfide isomerase. *Proc Natl Acad Sci USA* **90**, 2107–2111.